

CHAPTER 41

FETCH LIMITED SPECTRAL EVOLUTION IN FINITE DEPTH WATER

I.R. Young¹
L.A. Verhagen²

ABSTRACT

The results of a field experiment aimed at investigating the evolution of fetch limited waves in water of finite depth are presented. In particular, non-dimensional growth curves, the parametric form of the one dimensional spectrum and the directional spreading of the spectrum are investigated.

INTRODUCTION

Commencing with the cornerstone JONSWAP experiment (Hasselmann et al., 1973), the investigation of the evolution of deep water wind generated ocean waves has been a common theme. Although this case represents a very idealized situation, the resulting evolution provides valuable insight into the complex physics of wind wave evolution. In addition, the resulting non-dimensional growth curves and parametric spectral forms have proved a valuable aid to preliminary engineering design and for use in the validation of comprehensive spectral models.

The limitation of such studies to deep water is restrictive, particularly when it is considered that a significant percentage of coastal engineering works are in areas where finite water depth will influence the resulting wave field. Despite the obvious requirement, there exists no comprehensive counterpart to JONSWAP (Hasselmann et al., 1973) in finite depth water.

This paper presents the results of such an experiment. The evolution of the wave spectrum has been measured at a number of points along a shallow lake. The relatively simple geometry and bathymetry of the lake and the absence of contaminating swell results in a near ideal test basin in which to investigate fetch limited growth in finite depth water.

¹School of Civil Engineering, University College, UNSW, Canberra, ACT 2600, Australia

²Fugro-Inpark, P.O. Box 3000, 2260 DA Leidschendam, The Netherlands

The paper investigates three basic areas of finite depth fetch limited evolution: the development of non-dimensional energy and non-dimensional peak frequency with fetch, the one dimensional spectral form and directional spreading.

DESCRIPTION OF EXPERIMENT

The site chosen for the present experiment was Lake George (see Figure 1). The lake is approximately 20 km long by 10 km wide and has a relatively uniform bathymetry with an approximate water depth of 2 m. A series of 8 measurement stations were established along the long North-South axis of the lake as shown in Figure 1. With the exception of Station 6, the sites consisted of minimum blockage space frame towers, designed to provide minimum contamination to either wind or wave measurements made from the towers. The central site, Station 6, consisted of a large platform with temporary accommodation for the research team. Each of the sites was instrumented with a surface piercing Zwarts poles. In addition, cup anemometers at a reference height of 10 m were located at Stations 2, 4, 6, 7 and 8. Air temperature and relative humidity and water temperature were also measured at Stations 2, 6 and 8. A spatial array consisting of 7 Zwarts poles was established adjacent to the platform at Station 6 to provide high resolution measurements of the directional wave spectrum.

NON-DIMENSIONAL GROWTH CURVES

It is convenient to represent the data in terms of the non-dimensional variables: non-dimensional energy, $\epsilon = g^2 E / U_{10}^4$, non-dimensional frequency, $\nu = f_p U_{10} / g$, non-dimensional fetch $\chi = gx / U_{10}^2$ and non-dimensional depth $\delta = gd / U_{10}^2$ where g is gravitational acceleration, E is the total wave energy or variance of the wave record, f_p is the frequency of the spectral peak, d is the water depth, x is the fetch and U_{10} is wind velocity.

Figures 2 and 3 show scatter plots of ϵ (Figure 2) and ν (Figure 3) verses χ . The data have been partitioned into discrete intervals of δ . Figures 2 and 3 show data in the range $\delta = 0.2 - 0.3$. A preliminary investigation of the north/south data indicated that the data which conformed to deep water conditions was consistent with previous deep water growth law formulations. In particular, ϵ was well modeled by the JONSWAP relationship (Hasselmann et al., 1973), $\epsilon = 1.6 \times 10^{-7} \chi$ and ν by the Kahma and Calkoen (1992) form, $\nu = 2.18 \chi^{-0.27}$.

Noting these deep water asymptotic limits to the data, a nonlinear least squares analysis of the data yielded the model

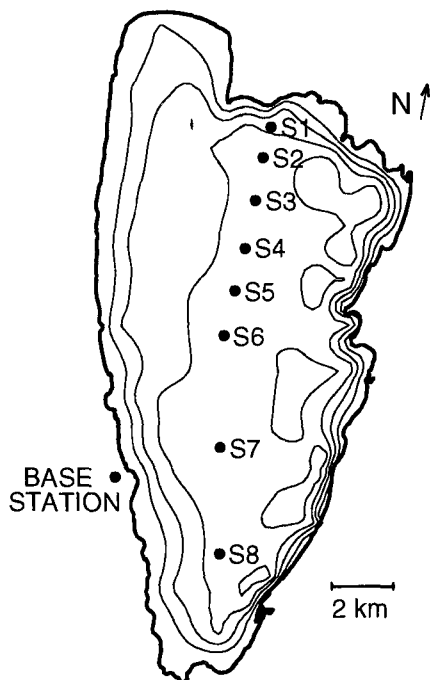


Figure 1: Map of the Lake George experimental site. The measurement locations are labelled S1 to S8. Data were transmitted to the Base Station on the western shore of the lake where it was logged under computer control. The contour interval is 0.5 m, with the maximum contour value 2 m.

$$\varepsilon = 3.64 \times 10^{-3} \left\{ \tanh A_1 \tanh \left[\frac{B_1}{\tanh A_1} \right] \right\}^{1.74} \quad (1)$$

where

$$A_1 = 0.493\delta^{0.75} \quad (2)$$

$$B_1 = 3.13 \times 10^{-3} \chi^{0.57} \quad (3)$$

and

$$\nu = 0.133 \left\{ \tanh A_2 \tanh \left[\frac{B_2}{\tanh A_2} \right] \right\}^{-0.37} \quad (4)$$

where

$$A_2 = 0.331\delta^{1.01} \quad (5)$$

$$B_2 = 5.215 \times 10^{-4} \chi^{0.73} \quad (6)$$

Equations (1) and (4) are shown in Figures 2 and 3 respectively. As these figures contains data for a finite range of δ (ie. $\delta = 0.2 - 0.3$), two curves are shown, one for each of the extremes of δ for that figure. Generally, the proposed

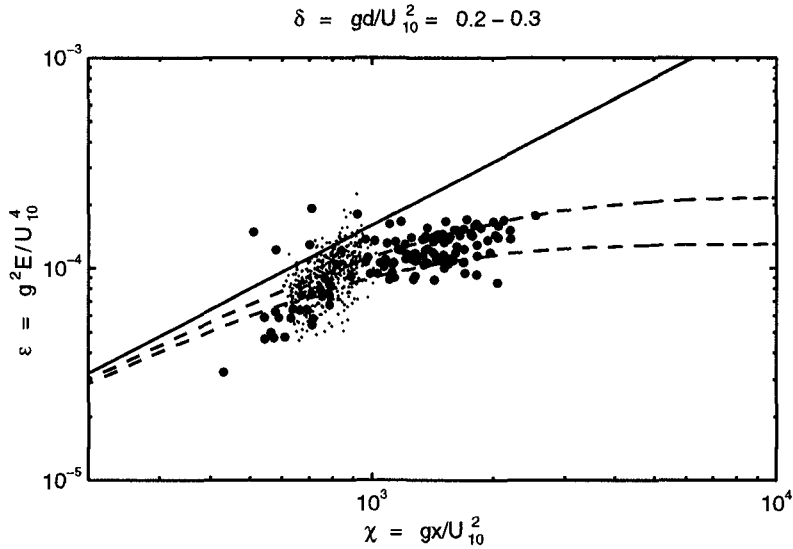


Figure 2: A scatter plot of non-dimensional energy, ϵ against non-dimensional fetch, χ . Only data with values of non-dimensional depth, δ between 0.2 and 0.3 are shown. The north/south data are shown as the large dots and the lower quality east/west data as the small dots. Equation (1) is shown for the two extremes of δ (ie. 0.2 and 0.3) by the two dashed lines. The deep water asymptotic form of Equation (1) is shown as the solid line.

relationships [(1) and (4)] approximate the data well. As with all previous field measurements of this type there is some data scatter.

At short non-dimensional fetch the waves are in deep water and approach the deep water asymptotic limits which are consistent with the numerous previous deep water data sets. As the non-dimensional fetch increases, the effects of the finite water depth become more pronounced and the data progressively deviate from the deep water limit. At relatively large values of non-dimensional fetch, further spectral development ceases as shown by the “plateau” regions of the curves in Figures 2 and 3. Rather than there being a single universal growth curve, there are a family of curves, one for each value of non-dimensional depth.

Lake George is approximately twice as long as it is wide and whether this aspect ratio limits the wave development along the north/south fetch must be addressed. To investigate this point, cases for which the wind direction was approximately perpendicular to the long east and west boundaries of the lake were extracted from the full data set. As there are no measurements of wind speed

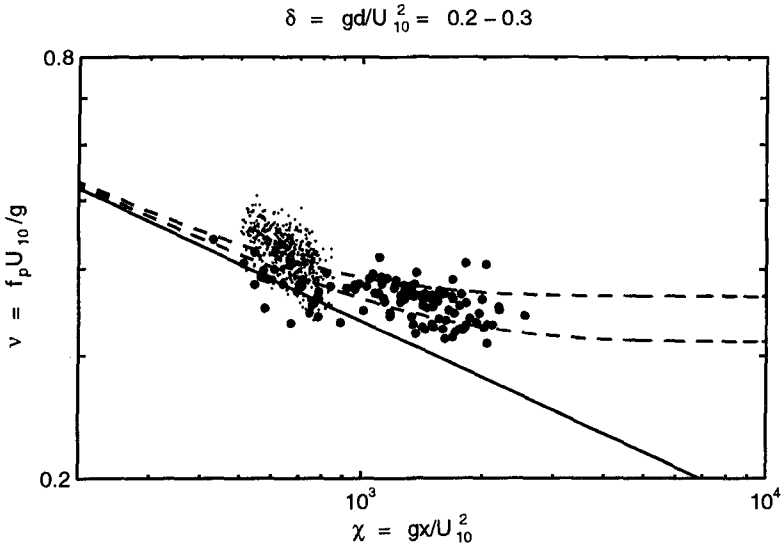


Figure 3: A scatter plot of non-dimensional peak frequency, ν against non-dimensional fetch, χ . Only data with values of non-dimensional depth, δ between 0.2 and 0.3 are shown. The north/south data are shown as the large dots and the lower quality east/west data as the small dots. Equation (4) is shown for the two extremes of δ (ie. 0.2 and 0.3) by the two dashed lines. The deep water asymptotic form of Equation (4) is shown as the solid line.

along the fetch for these cases, only data from Station 6, where the wind was always measured have been considered. As these east/west events are common, we can be very selective with the data, retaining only those cases for which the wind direction is within $\pm 10^\circ$ of normal to the respective shore lines. This east/west data set is also shown in Figures 2 and 3. Since there is no detailed information to determine the development of the wind field with fetch for these cases and since there is moderately elevated land to the east and west of the lake (compared with north/south which is quite flat) the east/west data set is considered to be of inferior quality to the north/south data set. Nevertheless, the east/west data set is consistent with the north/south data, confirming that the lake geometry has no significant influence on the results. It should be noted that there is only a relatively small range of values of χ for each selected range of δ for the east/west data, since all data is obtained from only a single dimensional fetch of approximately 5 km. Also, since the east/west data is believed to be of lesser quality than the north/south data, it was not used in the nonlinear least squares curve fit used to develop (1) and (4).

SPECTRAL EVOLUTION

Bouws et al. (1985) proposed the TMA spectral form for the representation of wind generated waves in water of finite depth

$$E(f) = \alpha g^2 (2\pi)^{-4} f^{-5} \exp \left[\frac{-5}{4} \left(\frac{f}{f_p} \right)^{-4} \right] \cdot \gamma \exp \left[\frac{-(f-f_p)^2}{2\sigma^2 f_p^2} \right] \cdot \Phi \tag{7}$$

and

$$\Phi = \left\{ \frac{[k(f, d)]^{-3} \frac{\partial k(f, d)}{\partial f}}{[k(f, \infty)]^{-3} \frac{\partial k(f, \infty)}{\partial f}} \right\} \tag{8}$$

Based on the wavenumber scaling arguments implicit in the TMA spectral form, Bouws et al. (1985, 1987) speculated that the spectral parameters should be functions of the non-dimensional wavenumber, $\kappa = U_{10}^2 k_p / g$, where k_p is the wavenumber of the spectral peak. To investigate this dependence with the present data set, the spectral parameters of α , γ and σ are presented as functions of κ in Figures 4, 5 and 6, respectively. As with previous studies of spectral evolution, there is significant scatter in the data.

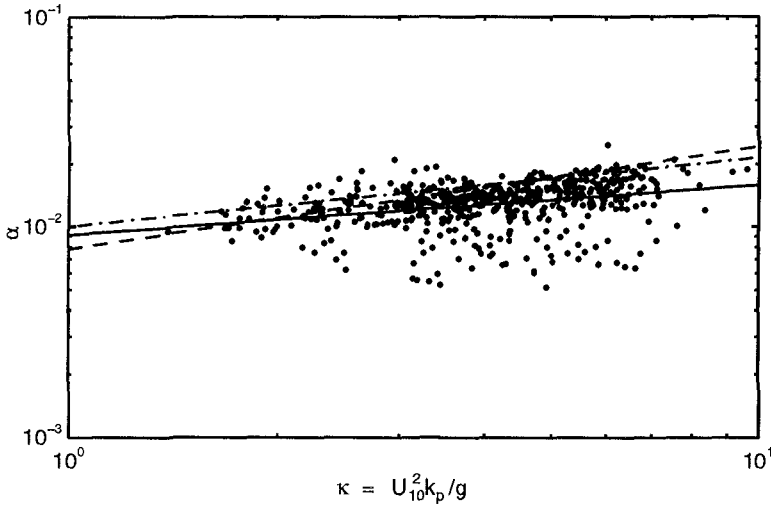


Figure 4: Values of the parameter α as a function of non-dimensional wavenumber, κ . The solid line is a least squares fit to the data [Equation (9)]. The TMA result is shown by the dashed line and the JONSWAP form, transformed from frequency to wavenumber space, by the dash-dot line.

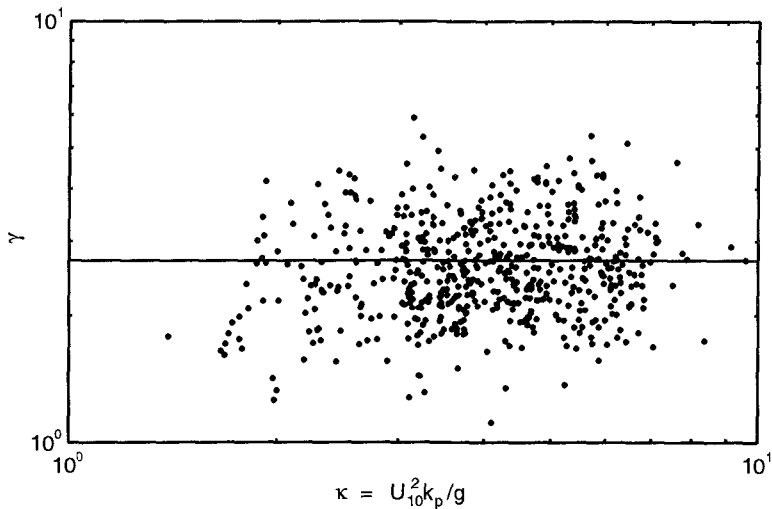


Figure 5: Values of the peak enhancement parameter, γ as a function of non-dimensional wavenumber, κ . The horizontal line represents the data mean.

Within the data scatter, a relationship between α and κ is clear, with α an increasing function of κ (see Figure 4). A least squares fit to the data yields the power law relationship

$$\alpha = 0.0091\kappa^{0.24} \quad (9)$$

Equation (9) is shown on Figure 4, together with the TMA result, $\alpha_{TMA} = 0.0078\kappa^{0.49}$. Both (9) and the TMA form are consistent with the data. In deep water the general TMA form reverts to that of JONSWAP. The deep water JONSWAP result scales α in terms of the non-dimensional frequency, ν , $\alpha_{JONSWAP} = 0.033\nu^{0.67}$. Assuming a deep water linear dispersion relationship, this result can be converted to wavenumber space, $\alpha_{JONSWAP} = 0.01\kappa^{0.33}$. This JONSWAP result is also shown in Figure 4 and is broadly consistent with the finite depth formulations.

All results are comparable and confirm that the trend towards decreasing values of α with increasing maturity of the waves, already observed in deep water, also holds in finite depth situations.

In contrast to the observable trend in α with κ , no similar result is apparent for either γ or σ . This result is consistent with both TMA (Bouws et al., 1985, 1987) and JONSWAP (Hasselmann et al., 1973). There is, however, significant sampling variability associated with these parameters. The mean values of the

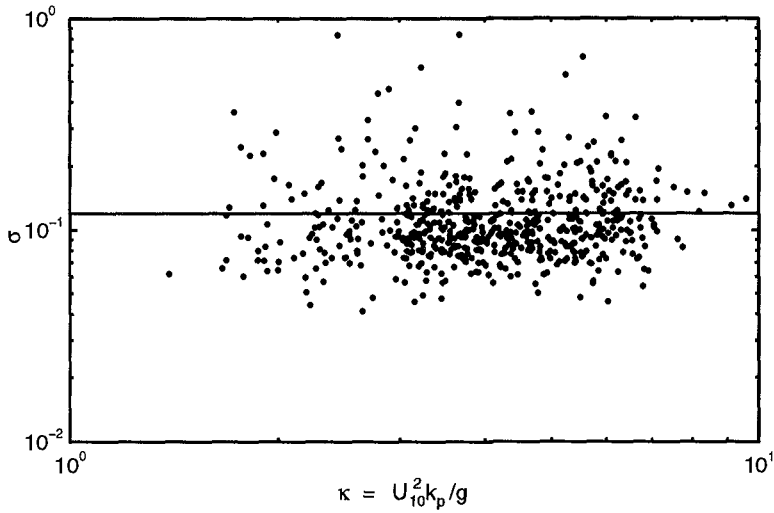


Figure 6: Values of the spectral parameter, σ as a function of non-dimensional wavenumber, κ . The horizontal line represents the data mean.

data set yield $\gamma_{mean} = 2.70$ and $\sigma_{mean} = 0.12$.

DIRECTIONAL SPREADING

Two common models have been proposed to represent the directional spreading of wind waves: $\cos^{2s} \theta/2$ and $\text{sech}^2 \beta \theta$. A number of different techniques have been reported for the fitting of such analytical forms to the data. Mitsuyasu et al. (1975) and Hasselmann et al. (1980) analyzed their buoy data using the Fourier Expansion Method (Longuet-Higgins et al., 1963; Young, 1994) and determined the value of s from the first 2 components of the Fourier expansion. Donelan et al. (1985) compared this approach with one in which the directional form was matched to the half-power points of the measured spreading function. It was argued that matching the half-power points was more meaningful since interest is concentrated on the energetic region of the directional distribution. This technique appeared to reduce the scatter in the data.

In addition to these techniques, application of a nonlinear least squares fit [Levenberg-Marquardt method, Press et al. (1986)] was also investigated with the present data. This least squares approach, was adopted here, together with a Maximum Likelihood Method analysis of the data from the directional array.

Both formulations of the spreading function yield qualitatively similar results,

indicating the spectrum is narrowest at the spectral peak frequency and broadens at frequencies both larger and smaller than the peak value. The $\cos^{2s} \theta/2$ formulation exhibited marginally less scatter than the $\text{sech}^2 \beta \theta$ form and was adopted for further analysis.

A least squares analysis of the directional data yields the following form for the present finite depth data

$$s = \begin{cases} 11 \left(\frac{f}{f_p}\right)^{2.7} & f < f_p \\ 11 \left(\frac{f}{f_p}\right)^{-2.4} & f \geq f_p \end{cases} \quad (10)$$

Equation (10) has been constrained to yield narrowest spreading at $f/f_p = 1$. The scatter in the data is such that the actual point of narrowest spreading cannot be determined with great accuracy. It is clearly, however, in the vicinity of the spectral peak frequency.

Equation (10) is shown in Figure 7 together with the deep water results of Mitsuyasu et al. (1975), Hasselmann et al. (1980) and Donelan et al. (1985). As the results of Mitsuyasu et al. (1975) and Hasselmann et al. (1980) are both wave age dependent, mean values typical of their respective data sets have been used to construct Figure 7 (Mitsuyasu et al., 1975 - $U_{10}/C_p = 1.1$; Hasselmann et al., 1980 - $U_{10}/C_p = 1.4$). As Donelan et al. (1985) provide no functional form expressed in terms of s , the result in Figure 7 was obtained from digitizing the result given in their Figure 30.

The present results are marginally narrower (higher s) than those of both Mitsuyasu et al. (1975) and Hasselmann et al. (1980), they are however significantly broader than the high resolution results of Donelan et al. (1985). As shown by Donelan et al. (1985), the results of both Mitsuyasu et al. (1975) and Hasselmann et al. (1980) are excessively broad due to the instrumentation and analysis technique utilized. The present result [Equation (10)] should have comparable resolving power to the result of Donelan et al. (1985). The inference is that finite depth wind wave spectra are broader than their deep water counterparts. Due to the relatively narrow range of $k_p d$ spanned by the present data set a more emphatic statement cannot be made. At present it is necessary to rely on these two independent data sets (Donelan et al., 1985 - deep water; Lake George - finite depth). There is always some possibility that, in addition to water depth, there are other unknown influences responsible for the different spreading.

CONCLUSIONS

The data set presented in this paper represents the first comprehensive field study of the evolution of fetch limited waves in water of finite depth. The data set is sufficiently comprehensive to fully define non-dimensional growth curves for both energy and peak frequency. In contrast to deep water results, a single growth relationship does not exist for each quantity. Rather, a family of curves result,

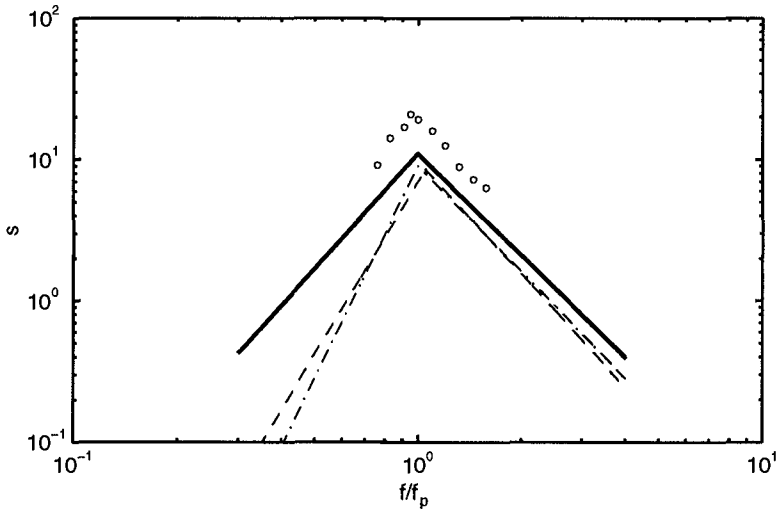


Figure 7: The dependence of the directional exponent s for the present finite depth data as a function of f/f_p [Equation (10)] (thick solid line). Also shown for comparative purposes are previous deep water data sets: Mitsuyasu et al. (1975) - 'dash dot line'; Hasselmann et al. (1980) - 'dashed line'; Donelan et al. (1985) - 'open circles'.

depending on the non-dimensional depth.

The one-dimensional spectrum has been shown to conform to the TMA form. The spectral parameter α is shown to be a function of the non-dimensional peak wavenumber, κ .

The directional spreading is qualitatively similar to deep water results. The spectra are narrowest at the spectral peak frequency and broaden at frequencies both above and below the peak. Compared with deep water results, finite depth spectra appear to exhibit broader spreading. This is possibly due to the different nonlinear coupling which will exist in finite depth cases.

The present data set is significantly more comprehensive than previous finite depth studies. The results of these previous studies are, however, consistent with the present results. This occurs, despite the fact that a wide range of bed materials exist for the various data sets. As a result, it can be speculated that bed material has little influence on spectral evolution under fetch limited conditions. This is markedly different to other finite depth cases, such as swell attenuation, where the rate of decay is very sensitive to the bed material.

REFERENCES

- Bouws, E., Günther, H., Rosenthal, W. and Vincent, C.L., 1985. Similarity of the wind wave spectrum in finite depth water, 1. Spectral form. *J. Geophys. Res.*, 90: 975-986.
- Bouws, E., Günther, H., Rosenthal, W. and Vincent, C.L., 1987. Similarity of the wind wave spectrum in finite depth water, 2. Statistical relationships between shape and growth stage parameters. *Dtsch. Hydrogh. Z.*, 40: 1-24.
- Donelan, M.A., Hamilton, J. and Hui, W.H., 1985. Directional spectra of wind-generated waves. *Phil. Trans. R. Soc. Lond.*, A 315: 509-562.
- Hasselmann, K. et al., 1973. Measurements of wind-wave growth and swell decay during the Joint North Sea Wave Project (JONSWAP). *Dtsch. Hydrogh. Z., Suppl. A*, 8, 12, 95pp.
- Hasselmann, D.E., Dunkel, M. and Ewing, J.A., 1980. Directional wave spectra observed during JONSWAP 1973. *J. Phys. Oceanogr.*, 10, 8: 1264-1280.
- Kahma, K.K. and Calkoen, C.J., 1992. Reconciling discrepancies in the observed growth of wind-generated waves. *J. Phys. Oceanogr.*, 22: 1389-1405.
- Longuet-Higgins, M.S., Cartwright, D.E. and Smith, N.D., 1963. Observations of the directional spectrum of sea waves using the motions of a floating buoy. in 'Ocean wave spectra', Englewood Cliffs, Prentice Hall, Inc.: 111-136.
- Mitsuyasu, H., Tasai, F., Suhara, T., Mizuno, S., Onkusu, M., Honda, T. and Rukiiski, K., 1975. Observations of the directional spectrum of ocean waves using a cloverleaf buoy. *J. Phys. Oceanogr.*, 5: 751-761.
- Press, W.H., Flannery, B.P., Teukolsky, S.A. and Vetterling, W.T., 1986. *Numerical Recipes*. Cambridge University Press, 818pp.
- Young, I.R., 1994. On the Measurement of Directional Wave Spectra. *Applied Ocean Research*, 16: 283-294.